

The onset of fluid invasion and flow development in a viscoplastic fluid

Marjan Zare¹, Ian Frigaard^{1,2}

¹ Mechanical Engineering, University of British Columbia, Vancouver, BC, Canada

² Department of Mathematics, University of British Columbia, Vancouver, BC, Canada

1 Abstract

During cementing of oil and gas wells, sufficiently over-pressured fluids may enter from the surrounding rock into a gelled cement slurry. This fluid invasion may lead to failure of well integrity. For Newtonian fluids, once the pore pressure balances the hydrostatic pressure and any capillary effect, invasion occurs. In contrast, yield stress fluids may remain stationary under the same pore pressure. We investigate the critical amount of over-pressure which is sufficient to overcome a combination of static pressure, yield stress and interfacial tension available in this problem.

2 Introduction

Gas migration has been a chronic problem in the cementing of oil and gas wells for decades. This is a complex phenomenon with causes that combine chemical, geochemical and fluid mechanical processes. The consequences of this problem can range from slow gas emissions at the wellhead or into the surrounding groundwater and ecological systems, through to well blowouts in extreme cases. Thus, the underlying costs of improper primary cementing include safety, environmental and economic aspects; see chapter 9 in [11] for a comprehensive review. In this paper we focus at what is called early-stage gas migration, i.e. when gas can enter the well before the cement slurry has set (fully hydrated). This is a fluid-fluid invasion process, in which the invading fluid is held in a porous medium, held back by the hydro-

static pressure of the cement slurry.

In order for fluid (gas or liquid) to invade it is necessary for there to be a pressure imbalance, i.e. formation pressure larger than hydrostatic pressure. In the case of a purely viscous fluid within the annulus, (neglecting capillary effects) a pressure over-balance is sufficient to ensure that formation fluid will enter the annulus. However, the cement slurry is generally characterized as a shear-thinning yield stress suspension, which also develops a gel strength during the early stages of hydration.

The flow considered in this paper is induced by invasion of a pressurized fluid through a centrally positioned hole in the wall at the bottom of a tall column of yield stress fluid (Carbopol solution). The applied pressure is gradually increased until invasion of the fluid occurs. In the first part of this study [18], we considered water as the invading fluid and observed a complex invasion process. In that study we explored the variation in invasion pressure with both yield stress and height of column. In the second part [17], we explored invasion pressure of a range of different invading fluids including miscible liquids and immiscible fluids. Over these two studies we have used water, glycerine, silicon oil and air.

We have not found any literature focused on the mechanism of invasion. Most of them study the cementing application about displacement/injection flows of yield stress fluids in pipes, both for miscible [1, 5, 15] and immiscible [2–4, 12, 16] scenarios. Invasion process is not the focus of these studies and for many the inlet is the entire pipe (duct), whereas here we have invasion only through a *small* hole. Germanovich and co-authors [6, 7] studied inva-

sion and fracturing of soft rocks with viscous fluids, (in these the focus is on fracture propagation and morphology). Others have looked at similar flows in Hele-Shaw cell geometry e.g. [8, 9, 13]. Although the later parts of our experiments do exhibit viscous fingering type phenomena, as in these studies, our focus is on the preceding invasion stage and not the propagation.

An outline of our paper is as follows. The experimental method is outlined in §3 along with the properties and rheology of invading and invaded fluids. Our experimental results are presented in three sections: invasion process of miscible fluids (§4) and immiscible fluids (§5) and invasion pressures (§6). The paper ends with a brief discussion about the findings of this study in §7.

3 Experimental method

Consider the following simplified setup in which fluid invasion can occur. A long plexiglas cylinder of radius $\hat{R} = 3.175$ cm (1.25") and length $\hat{L} = 63.5$ cm (25") contains the yield stress fluid up to the height \hat{H} . For the experiments in which, $\hat{H} < \hat{L}$, the space above the yield stress fluid is filled to height \hat{H}_C with water so that, regardless of height of the yield stress fluid, the total height of liquid (and static head) in the cylinder is constant between experiments. To minimize the optical distortion, the cylinder is placed inside a the rectangle tank and space between them is filled with a glycerin solution that has a refractive index close to that of plexiglas. In order to avoid wall slip of carbopol macrogels on plexiglas sheet, the inner surface of the cylinder is treated with a PEI solution, following the method suggested by Métivier et al. [10].

The injection path is a hole of radius $\hat{R}_h \approx 0.32$ mm ($r_h \approx 0.01$) embedded in the base of the cylinder. The invading fluid moves into the hole through a connecting tube between the cylinder and reservoir that is placed on top of a motorized scissor jack, i.e. a manometer design; see Fig. 1. The pressure exerted within

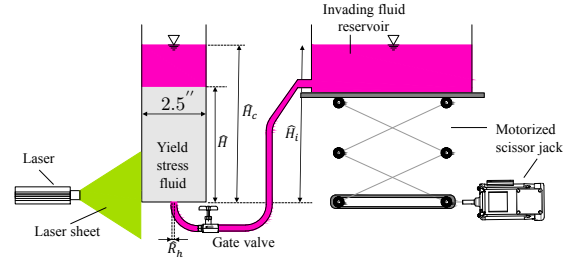


Figure 1. Schematic of the experimental setup.

the invading fluid \hat{P}_h is given by the difference in static pressures of the two fluid columns. Atmospheric pressure is balanced and in this static configuration the invading pressure can be resisted only by yield stress effects and (potentially) surface tension effects.

Initially, the water and carbopol tanks are positioned at the same level such that the hydrostatic pressure is balanced between them. The surface height in both tanks is measured by using a laser level projecting onto a scale giving pressure to within 5 Pa. The experiment procedure is such that the applied pressure within the invading fluid “pore” gradually increases until the fluid enters the column. The height change can be controlled with the precision of $0.1 \mu\text{m}$, which equals a static pressure of $\approx 0.001\text{Pa}$ as the resolution of our system during increasing pressure within the invading fluid.

The planar Laser-Induced Fluorescence (planar-LIF) technique is used to identify the entry of the fluid once invasion occurs. Red fluorescence powder, which has maximum excitation upon contact with 532nm green laser light, is used to dye the invading fluid. The experiments are recorded using two cameras. A JAI AD-081 (Edmunds OPTICS) with 16mm compact Fixed Focal Length Lens is used to record a small field of view of $2.5 \times 3\text{cm}^2$, around the hole with a spatial resolution of ≈ 30 pixels per mm. The second camera (Nikon D800) records flow propagation with 720 pixel resolution with 60 frames per second, giving a spatial resolution of $\approx 10 - 15$ pixels per mm.

3.1 Invading and host fluids

The in-situ yielded stress fluid is a solution of Carbopol EZ-2 (Lubrizol). Carbopol is a common water-based yield stress material used in many different applications. The rheology of this material and specifically its yield stress is mainly a function of the concentration, pH, and preparation procedure. To prevent time-dependency of the material, we used an identical procedure for our Carbopol preparation and it was prepared daily for the experiments of the same day. The desired concentration of Carbopol powder was mixed with water for one hour, then it was neutralized by stirring in an appropriate amount of 0.1 g/l of sodium hydroxide solution (*NaOH*), and then mixed for 23 hours.

The range of Carbopol concentrations in our experiments was: 0.15-0.17%wt. We took 3 to 4 samples from each batch of Carbopol to measure the rheology. The yield stress was measured using a Gemini HR nano rheometer (Malvern Instruments). A parallel plates geometry was used and the stress at 100 data points was collected during the test. The sandpaper with the roughness of 400 is stuck on the plates to suppress wall slip effects Carbopol. The test was performed by controlling the shear rates and allowing it to ramp up from 0.001s^{-1} to 0.1s^{-1} with a recovery time of 7 seconds on each step of ramp. The yield stress was estimated using the maximum viscosity method, as has been used before for Carbopol solutions [14]. This method assumes that when the material yields it has the maximum effective viscosity. The yield stress values of carbopol solution used in our experiments are in the range of 5.1 – 10 Pa.

Two sets of fluids, miscible and immiscible, are used as invading fluids. The invading fluids were all Newtonian and the range of fluids is designed to tackle the effect of each single parameter: viscosity, density difference and interfacial tension. The three miscible fluids are injected into Carbopol were: water (**H₂O**), glycerin 45 % (**G45**), and glycerin 58% (**G58**). Two immiscible fluids were used: Rhodorsil oil

Table 1. Physical properties of the invading liquids.

	H₂O	G45	G58	R550
$\hat{\rho}$ [g/cm ³]	1	1.06	1.12	1.065
$\hat{\mu}$ [cP]	1	4.9	9.8	125

(BLUESIL FLD 550 from Bluestar Silicones; **R550**) and air. The physical properties of these liquids are given in Table 1. On injecting the **R550**, the objective was to isolate the effect of interfacial tension on invasion. Consequently, for these experiments the Carbopol density was increased by weighting with glycerin, to match that of the invading fluid.

4 Invasion process of miscible fluids

To explore the invasion process we varied \hat{H} and $\hat{\tau}_y$ for each invading fluid. Three carbopol concentrations, 0.15, 0.16 and 0.17%wt, and five heights of yield stress fluid were used: $H = \hat{H}/\hat{R} = 2, 5, 10, 15, 20$. Aiming for consistency of the results, each test was repeated 3-5 times, and in total we performed around 60 experiments for each fluid. The invasion/penetration of the miscible fluids into Carbopol, namely flow yielding/initiation, is characterized by the following stages.

1. *Mixing stage*: A very small mixed region of water/carbopol develops directly above the hole. The water is observed to mix into the carbopol, but there is no observable motion of the fluids (i.e. no displacement). This stage is probably driven by molecular diffusion, or perhaps osmosis. If the pressure is not increased further, this small mixing region will become progressively diffuse.
2. *Invasion stage*: At the center of the mixed region, when the pressure is high enough, the water advances into mixed region of the carbopol column (Invasion). Typically the invasion takes the form of a minuscule dome appearing, ($\approx 0.5 - 0.7\text{mm}$ ra-

Table 2. The averaged of maximum dome radii after invasion

	H₂O	G45	G58
\hat{R}_d [mm]	1.45±0.15	2.46±0.27	2.07±0.27

dius), in which the intensity of the LIF image is significantly brighter than in the diffuse mixing stage and is observed to oscillate and becomes significantly brighter. That’s when the applied pressure is held constant. These phenomena signify the onset of a second stage of the invasion, that we have called it transition. In which the small dome formed at the invasion stage grows larger. The maximum size of domes varies by invading fluid but doesn’t have a coherent trend with concentration and height. They are averaged over the data obtained during a series of repetitive experiments which were done for each fluid, and the results are reported in Table. 2.

During the transition process, although there is a flow into the dome from the reservoir, the change in static pressure balance is negligible and the over-pressure can be regarded as constant.

3. *Fracture stage:* After the invasion, a “fracturing” stage occurs. A small finger initiates the fracture of the Carbopol and the water advances ahead of the dome in a dyke-like sheet that tends to finger and branch as it advances. Figures 2 a) & b) display images taken of the **G45** and **H₂O** dykes after fracture.
4. *Arrest stage:* Since the applied pressure is not increased anymore, the flow eventually stops. The fluids stop as static equilibrium is attained. In the case of water invasion, the arrest height is dependent on the Carbopol height $H(= \frac{\hat{H}}{\hat{R}})$. Either the invading water penetrates fully to the surface of the Carbopol (commonly when $H = 4, 10$) or it stops before reaching the surface ($H = 20$). In the case where the fingers/fractures stop before reaching the sur-

face, the final height effectively indicates a “fracture” pressure. By comparison, the glycerin dykes tend to rotate around the tube and rise up only very slightly, which can be attributed to the higher density of glycerin to that of carbopol.

5 Invasion process of immiscible fluids

Two immiscible fluids, rhodorsil oil (**R550**) and air, were injected into the carbopol column.

Rhodorsil oil (R550) : This fluid is very viscous and slightly more dense than carbopol. Density and viscosity of **R550** are listed in Table 1. With aiming to isolate the effect of surface tension on the invasion pressure, the density of the carbopol solution is increased to match that of rhodorsil oil, by using a low concentration glycerin solution to increase density. It is observed that interfacial tension prevents the formation of the initial mixing regime observed in miscible fluids invasion, (again confirming its molecular diffusive origin). Therefore, we do not see the small diffuse penetration and nor the oscillatory motion of the mini-dome signalling the “invasion point”. Instead **R550** emerges as a dome into the column of yield-stress fluid and then it expands very slowly. Due to high viscosity of this fluid, it takes some hours until it displaces around 5 – 8 cm of the column of the carbopol. As here there is no localization of the invasion nor any mixing, the steady increase of dome volume results in displacement upwards of the Carbopol column. An example of flow development after invasion of **R550** is shown in Figure 2.c.

Air: Compared to **R550** the interfacial tension was increased by a factor of 2-3, but air also has a far smaller viscosity and density. Similar to **R550**, the onset is quite localised, with no mixing and an initial (approximately) hemispherical expansion. However, relatively rapidly the effect of buoyancy appears to dominate and the radius of the invading air column in fact contracts from a maximum, then pinches off from the hole and rises in as a bubble.

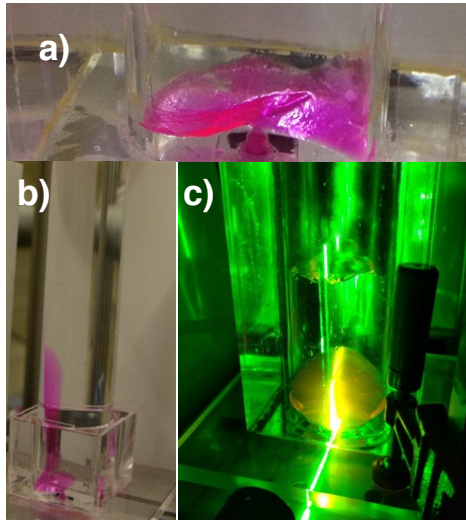


Figure 2. Sample snapshots of flow development after invasion of a) **G45** b) **H₂O** c) **R550**

It must be mentioned that the invasion/bubble growth and pinch off all occur at the same imposed pressure, i.e. once invasion starts the process continues through to detachment relatively rapidly. Evidently, the effect of surface tension decreases as the bubble expands and buoyancy also contributes to this accelerating process.

6 Invasion pressure

From a naïve macroscopic perspective, we may expect a linear increase of invasion pressure with height of the column. Assuming that the material is incompressible, it is necessary for the invading fluid to displace fluid throughout the gelled column, i.e. volume is conserved. In this scenario, a yield surface must extend to surface and hence the invasion pressure should approximately scale with H .

The recorded invasion pressures, \hat{P}_i , are scaled and used to give an experimental measurement of the dimensionless invasion pressure. These are plotted against the scaled height of the column of carbopol, H , in Fig. 3. **R550**, **Air**, **G58**, **G45** & **H₂O** are respectively marked with a (\blacktriangledown , \blacklozenge , \blacksquare , \bullet , \blacktriangle).

Here our focus is on the difference between invasion pressures of miscible and immiscible

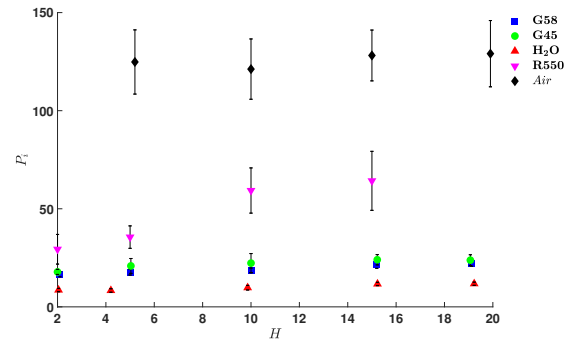


Figure 3. Invasion pressures of miscible and immiscible fluids against height of the carbopol column: \blacktriangledown **R550**, \blacklozenge **Air**, \blacksquare **G58**, \bullet **G45**, and \blacktriangle **H₂O** [18].

ble fluids qualitatively. Miscible fluids weaken the gel due to molecular diffusion or osmosis mechanism which results to a lower invasion pressures in comparison with values obtained for immiscible ones. The increase in the P_i against H is lower than what could be estimated by assuming that the whole column is yielded, $\sim 2H$. This suggests that for **H₂O**, **G45** & **G58** the stress field and yielding associated with invasion are strongly localized.

Our experiments with immiscible fluids involved a density matched silicon oil (**R550**) and air. It was clear that interfacial tension had a large effect on invasion. The invasion pressure was significantly larger than for the glycerin solutions and was non-local such that it was resisted by yielding at the walls of the column, with P_i increasing as the Poiseuille flow $\sim 2H$. Although air did not mix and had no micro-invasion dome, but the invasion was localised. The air invasion was buoyancy dominated and resistance of invasion at the walls did not occur. Therefore, P_i was approximately constant with H . Also P_i was much larger for air than for **R550**. Further analysis of this increased P_i suggested that about 50% of P_i is directly attributable to interfacial tension and the remainder to yield stress; see [17]. However, the yield stress is only able to resist effectively because there is no mixing/difusion.

7 Conclusions

We have presented results obtained from an experimental study of the invasion of miscible and immiscible fluids into a gelled static column of yield stress fluid. We observed that interfacial tension plays a significant role in both the invasion process and pressures. We find that the pressures required to initiate miscible fluid invasion are significantly lower than those triggering the invasion of immiscible fluids. The reason lies in the fact that for miscible fluids there is an initial diffusive mixing stage which facilitates their local penetration. Viscosity potentially retards this stage: more viscous invading fluids require larger invasion pressures. The immiscible liquid penetrates in the form of a slowly expanding dome, resisted at the walls of the column: effectively by a Poiseuille flow above it in the Carbopol column. The pressure required to initiate gas invasion is influenced approximately equally by interfacial tension and yield stress.

8 Acknowledgements

This research has been carried out at the University of British Columbia, supported financially by the Petroleum Technology Alliance Canada through project 16-WARI-02 funded under the Alberta Upstream Petroleum Research Fund Program. Part funding was also provided by NSERC and Schlumberger through CRD project 444985-12. The authors thank Linus Gassmann and Andrew Dworschak for assisting in running experiments.

References

- [1] K. Alba, S. M. Taghavi, J. R. de Bruyn, and I. A. Frigaard. *J. Non-Newtonian Fluid Mech.*, 201:80–93, 2013.
- [2] D. A. de Sousa, E. J. Soares, R. S. de Queiroz, and R. L. Thompson. *J. Non-Newtonian Fluid Mech.*, 144(2-3): 149–159, 2007.
- [3] P. R. de Souza Mendes, E. S. S. Dutra, J. R. R. Siffert, and M. F. Naccache. *J. Non-Newtonian Fluid Mech.*, 145(1): 30–40, 2007.
- [4] Y. Dimakopoulos and J. Tsamopoulos. *J. Non-Newtonian Fluid Mech.*, 112(1): 43–75, 2003.
- [5] C. Gabard. PhD thesis, Thèses de doctorat de l’Université Pierre et Marie Curie, Orsay, France, 2001.
- [6] L. N. Germanovich, R. S. Hurt, J. A. Ayoub, E. Siebrits, D. Norman, I. Ispas, C. T. Montgomery, et al. In *SPE International Symposium and Exhibition on Formation Damage Control*, 2012.
- [7] R. S. Hurt, L. N. Germanovich, et al. In *SPE Annual Technical Conference and Exhibition*, 2012.
- [8] A. Lindner, P. Coussot, and D. Bonn. *Phys. Rev. Lett.*, 85(2):314, 2000.
- [9] A. Lindner, P. Coussot, and D. Bonn. *Branching in Nature*. Springer, 2001.
- [10] C. Métivier, Y. Rharbi, A. Magnin, and A. Bou Abboud. *Soft Matter*, 8(28): 7365–7367, 2012.
- [11] E. B. Nelson. *Well cementing*. Schlumberger, 2006.
- [12] A. J. Poslinski, P. R. Oehler, and V. K. Stokes. *Polym. Eng. Sci.*, 35(11): 877–892, 1995.
- [13] N. Puff, G. Debrégeas, J.-M. Di Meglio, D. Higgins, D. Bonn, and C. Wagner. *Europhys. Lett.*, 58(4):524, 2002.
- [14] P. R. Souza Mendes and E. S. S. Dutra. *Appl. Rheol.*, 14(6):296–302, 2004.
- [15] S. M. Taghavi, K. Alba, M. Moyers-Gonzalez, and I. A. Frigaard. *J. Non-Newtonian Fluid Mech.*, 167: 59–74, 2012.

- [16] R. L. Thompson, E. J. Soares, and R. D. A. Bacchi. *J. Non-Newtonian Fluid Mech.*, 165(7-8):448–452, 2010.
- [17] M. Zare and I. A. Frigaard. *Submitted to Phys. Fluids and under revision.*, 2018.
- [18] M. Zare, A. Roustaei, K. Alba, and I. A. Frigaard. *J. Non-Newtonian Fluid Mech.*, 238:212–223, 2016.